Sox9+ ductal cells are multipotent progenitors throughout development but do not produce new endocrine cells in the normal or injured adult pancreas

Janel L. Kopp*, Claire L. Dubois*, Ashleigh E. Schaffer, Ergeng Hao, Hung Ping Shih, Philip A. Seymour, Jenny Ma and Maike Sander†

SUMMARY

One major unresolved question in the field of pancreas biology is whether ductal cells have the ability to generate insulin-producing β-cells. Conclusive examination of this question has been limited by the lack of appropriate tools to efficiently and specifically label ductal cells in vivo. We generated *Sox9CreER^T2* mice, which, during adulthood, allow for labeling of an average of 70% of pancreatic ductal cells, including terminal duct/centroacinar cells. Fate-mapping studies of the Sox9+ domain revealed endocrine and acinar cell neogenesis from Sox9+ cells throughout embryogenesis. Very small numbers of non-β endocrine cells continue to arise from Sox9+ cells in early postnatal life, but no endocrine or acinar cell neogenesis from Sox9+ cells occurs during adulthood. In the adult pancreas, pancreatic injury by partial duct ligation (PDL) has been suggested to induce β-cell regeneration from a transient Ngn3+ endocrine progenitor cell population. Here, we identify ductal cells as a cell of origin for PDL-induced Ngn3+ cells, but fail to observe β-cell neogenesis from duct-derived cells. Therefore, although PDL leads to activation of Ngn3 expression in ducts, PDL does not induce appropriate cues to allow for completion of the entire β-cell neogenesis program. In conclusion, although endocrine cells arise from the Sox9+ ductal domain throughout embryogenesis and the early postnatal period, Sox9+ ductal cells of the adult pancreas no longer give rise to endocrine cells under both normal conditions and in response to PDL.

KEY WORDS: Sox9, Pancreas, Regeneration, Multipotent progenitor, Neogenesis, Partial duct ligation, Mouse

INTRODUCTION

All pancreatic cell types, which encompass five different endocrine lineages as well as the exocrine acinar and ductal cells, are derived from a pool of early pancreatic progenitor cells that express the transcription factors Pdx1, Ptf1a and Sox9 (Gu et al., 2002; Kawaguchi et al., 2002; Akiyama et al., 2005). During subsequent development, the expression of Ptf1a and carboxypeptidase 1 (Cpa1) becomes restricted to cells in the tips of the branching epithelium, whereas markers such as Nkx6.1, Sox9 and Hnf1b become exclusively localized to the trunk portion of the organ (Seymour et al., 2007; Zhou et al., 2007; Solar et al., 2009; Schaffer et al., 2010). During the secondary transition, which marks the major wave of endocrine cell differentiation between embryonic day (e) 13.5 and e16.5 (Pictet and Rutter, 1972), transient endocrine precursor cells marked by Ngn3 (Neurog3 – Mouse Genome Informatics) arise from the Sox9+ Hnf1b+ early ducts (also called embryonic cords) in the trunk and give rise to the endocrine cells of the postnatal pancreas (Seymour et al., 2008; Solar et al., 2009). Lineage

tracing experiments of Hnf1b+ cells demonstrated that the embryonic cords generate endocrine and duct cells but not acinar cells (Solar et al., 2009). Based on these findings it has been suggested that acinar cell expansion after e13.5 is solely based on acinar cell proliferation and not on neogenesis.

The question of whether or not the adult pancreas contains facultative progenitors capable of generating endocrine cells during postnatal life has been highly controversial. Pulse-chase experiments based on genetic lineage labeling of insulin+ β-cells have suggested that postnatal β-cell mass expansion is entirely based on self-duplication of pre-existing β-cells (Dor et al., 2004). Accordingly, direct lineage labeling of the Hnf1b+ ductal or the mucin-1+ ductal/acinar cell compartment failed to demonstrate a contribution of exocrine cells to the endocrine compartment after birth (Solar et al., 2009; Kopinke and Murtaugh, 2010). Although these studies suggest that endocrine cells do not arise from ducts during normal aging, they do not exclude the possibility that the adult pancreatic ductal tree contains facultative endocrine progenitors. Consistent with the idea that such progenitors exist, centroacinar or terminal duct cells, which express Sox9 and lie at the interface of acini and small ducts, were found to be competent of endocrine cell differentiation when injected into fetal pancreatic explants (Rovira et al., 2010). Moreover, based on the observation that small clusters of endocrine cells accumulate close to the ducts in models of pancreatic injury, it has been suggested that injury activates an endocrine neogenic program in facultative ductal progenitors (Gu and Sarvetnick, 1993; Wang et al., 1996; Xu et al., 1999). Further supporting this notion, a recent study found pancreatic injury by PDL to be associated with the appearance of

Department of Pediatrics and Cellular and Molecular Medicine, University of California-San Diego, La Jolla, CA 92093-0695, USA.

*These authors contributed equally to this work
†Author for correspondence (masander@ucsd.edu)

Ngn3^{+} cells in small ductules (Xu et al., 2008). However, as Ngn3 is also expressed in endocrine cells of the adult pancreas (Wang et al., 2009), the lineage relationship between ducts, Ngn3^{+} cells and β-cells after PDL has remained unclear.

By employing genetic lineage tracing approaches, two studies have recently begun to address whether ductal cells contribute to the β-cell compartment after PDL. Using a 1.6 kb human *carbonic anhydrase II* (*CAII*) promoter fragment to direct expression of a tamoxifen (TM)-inducible form of Cre recombinase (CreER[TM]) to pancreatic ducts in mice, Inada et al. observed lineage-labeled β-cells (Inada et al., 2008), suggesting that ducts could give rise to new β-cells. However, as the expression of the *CAIICreER* transgene was not fully characterized and the overall percentage of labeled β-cells was not quantified before and after PDL, the validity of this positive finding is in question. Contrary to the findings by Inada et al., a bacterial artificial chromosome (BAC) transgenic approach for tracing Hnf1b^{+} ductal cells failed to detect duct-derived β-cells after PDL (Solar et al., 2009). However, because only a small portion of ductal cells were labeled by the *Hnf1bCreER* transgene (Solar et al., 2009), it has been suggested that a population bias accounts for these negative findings (Kushner et al., 2010).

Owing to the unique expression of Sox9 in various stem/progenitor cell compartments (Cheung and Briscoe, 2003; Vidal et al., 2005; Seymour et al., 2007; Garcia-Lavandeira et al., 2009), including the endocrine differentiation-competent terminal duct cells of the adult pancreas (Rovira et al., 2010), we examined the developmental potential of the Sox9^{+} domain in vivo. To trace cells that originate from the embryonic and adult Sox9^{+} domain, we generated BAC transgenic mice that express CreER[T2] under control of *Sox9* regulatory sequences. We show that the Sox9^{+} cell compartment remains multipotent until birth, giving rise to endocrine, acinar and duct cells. Furthermore, Sox9^{+} cells continue to produce small numbers of non-β endocrine cells until three weeks after birth. We further demonstrate that Ngn3 becomes activated in cells arising from the Sox9^{+} domain after PDL, but observed no contribution of these cells to the β-cell population, suggesting that PDL does not induce appropriate signals for the differentiation of duct-derived Ngn3^{+} cells into β-cells.

MATERIALS AND METHODS

Mice
To generate *Sox9CreER[T2]* mice, we modified the RP23-229L12 BAC clone by inserting the KOZAK-*CreER[T2]*-polyA sequence in place of the ATG start codon of the *Sox9* open reading frame in exon 1. BAC DNA was injected into the pro-nucleus of fertilized CB6F2 oocytes (UC Irvine Transgenic Mouse Facility, CA, USA). *R26R[lacZ]* and *R26R[YFP]* mice have been described previously (Soriano, 1999; Srinivas et al., 2001). Mice were maintained on a 70% CD1 (Charles River, MA, USA) and 30% C57BL/6 (Charles River) background. Tamoxifen (Sigma, St Louis, MO) was dissolved at 20 mg/ml in corn oil (Sigma) and administered intraperitoneally to pregnant females (2 mg per 40 g body weight) or subcutaneously to postnatal mice (5 mg per 40 g body weight). Partial duct ligation (PDL) was conducted as described (Xu et al., 2008; Chung et al., 2010). All animal experiments described herein were approved by the University of California, Irvine and San Diego Institutional Animal Care and Use Committees.

Histology and immunostaining
β-Galactosidase detection and subsequent paraffin embedding of tissue was performed as previously described (Seymour et al., 2004). Whole-mount pancreata were dehydrated and then cleared with BABB (1:2 benzyl alcohol to benzyl benzoate) for visualization.

Processing of tissues, Hematoxylin and Eosin (H&E) staining and immunohistochemistry were performed as described (Seymour et al., 2008). Additional blocking of mouse antigens using the M.O.M. Kit (Vector, Burlingame, CA, USA) was carried out for primary mouse antibodies. Immunodetection of Hes1 and Hnf1b required amplification of the primary signal using the TSA Kit (Invitrogen, Carlsbad, CA, USA) or the use of biotinylated secondary antibodies, respectively. For co-staining experiments using the rabbit anti-Ptf1a and rabbit anti-Sox9 antibodies, the Zenon Kit (Invitrogen) was used. A complete list of primary and secondary antibodies and their dilutions is shown in Table 1. Biotinylated *Dolichos biflorus* agglutinin (DBA), which binds to lectins present on ductal cells, was obtained from Vector Laboratories and used at 1:500.

Tissue sections were viewed on a Zeiss Axio Observer microscope. Images were captured with the ApoTome module and an Axiocam HRc Rev 3 color or Axiocam MRm Rev 3 monochrome digital camera driven by Zeiss Axiovision 4.8 software and processed using Photoshop CS4.

Quantitative real time PCR analysis (qRT-PCR)
Pancreatic heads and tails of PDL-treated and sham-operated mice were separated at the suture or projected position of the suture. For cell sorting, tissue was first dissociated at 37°C with 1.8 mg/ml collagenase B (Roche, Basel, Switzerland), then with 0.25% trypsin EDTA (Invitrogen), passed through a 35 μm filter (BD Biosciences, San Jose, CA, USA) and sorted on a FACSAria II (BD Biosciences). Cells from four mice per group were individually isolated and cells from two mice from each group were pooled after sorting.

Islets from pancreatic heads and tails of six PDL-treated and whole pancreata of six sham-operated mice were isolated by intraductal injection of 0.5 mg/ml Liberase (Roche), purified on a Histopaque-1077 (Sigma) gradient, hand-picked under a microscope and pooled for each experimental group.

Tissues or cells were lysed in equal final volumes of RLT buffer (Qiagen, Valencia, CA, USA). Total RNA was isolated with the Qiagen Micro RNA Extraction Kit and RNA concentration measured using a Nanodrop spectrophotometer. For RNA isolated from pancreatic heads and tails, cDNA was prepared using the Superscript III cDNA Synthesis Kit (Invitrogen) and qPCR analysis performed using the Power SYBR Green PCR master mix (Applied Biosystems, Carlsbad, CA, USA). For sorted cells and isolated islets, the Power SYBR Green RNA-to-C_T[TM] 1-Step Kit (Applied Biosystems) was used for qRT-PCR analysis. For detection of *Sox9* and *Ngn3* mRNA, 5 ng and 30 ng of total RNA were used in each reaction, respectively. Reactions were performed in duplicates. Primers used were: Sox9, 5′-AGACTCACATCTCTCCTA-ATGCT-3′ and 5′-ACGTCGGTTTTGGGAGTGG-3′; and Ngn3, 5′-AATGATCGGGAGCGCAATCG-3′ and 5′-CGCAGGGTCTCGA-CCTTTG-3′. Analysis of the data was performed using the comparative ΔCt method, as described (Pfaffl et al., 2001).

Insulin ELISA assay
For insulin measurements, whole ligated or unligated pancreata were homogenized in equal final volumes of acid ethanol. Insulin content of these extracts was measured by mouse insulin ELISA (Alpco Diagnostics, Salem, NH, USA) (Seymour et al., 2008). Total insulin content of each pancreas was normalized by dividing total insulin protein per pancreas by body weight of the mouse.

Morphometric analysis and cell counting
For morphometric analyses, the entire embryonic or adult pancreas was sectioned and evenly distributed 10 μm sections throughout the organ were selected. Four sections (~5% of the pancreas) in embryos, three sections (~2% of the pancreas) in juvenile mice and four sections (~1.25% of the pancreas) in adult mice were analyzed.

Recombination efficiencies were quantified by dividing the number of Sox9^{+} and YFP^{+} cells by the total number of Sox9^{+} cells in nine random fields of view from three sections per mouse. To determine the specificity of CreER expression, we examined all CreER^{+} cells on three sections per lineage marker (insulin, glucagon, pancreatic polypeptide, somatostatin, amylase) at e14.5, e18.5 and postnatal day (P) 25.

Table 1. Antibodies used for immunohistochemistry

Antigen	Species	Source	Dilution
		Primary antibodies	
Sox9	Rabbit	Chemicon	1:1000
Sox9	Goat	Santa Cruz	1:500
Cre	Mouse	Chemicon	1:1000
Glucagon	Guinea Pig	Dakocytomation	1:5000
Glucagon	Goat	Santa Cruz	1:1000
Glucagon	Mouse	Sigma	1:5000
Insulin	Mouse	Sigma	1:5000
Insulin	Guinea Pig	Dakocytomation	1:1000
Pancreatic polypeptide	Rabbit	Dakocytomation	1:2000
Somatostatin	Mouse	SOMO18, Beta Cell Biology Consortium (BCBC), Denmark	1:2000
Somatostatin	Rabbit	Dakocytomation	1:3000
Ptf1a	Rabbit	B. Breant, INSERM-Paris, France	1:1000
Hnf1b	Goat	Santa Cruz	1:100
Amylase	Rabbit	Sigma	1:500
Ngn3	Guinea Pig	Henseleit et al. (2005)	1:1000 in adult 1:2000 in embryo
GFP	Rat	C. Kioussi, Oregon State University, OR, USA	1:1000
Pdx1	Guinea Pig	C. Wright, Vanderbilt University, TN, USA	1:10,000
Pdx1	Goat	C. Wright, Vanderbilt University, TN, USA	1:100,000
Nkx6.1	Mouse	clone 2023, BCBC, Denmark	1:500
Pax6	Rabbit	Chemicon	1:1000
Mucin-1	Armenian hamster	Lab Vision	1:200
Osteopontin	Goat	R&D Systems	1:1000
Hes1	Rabbit	T. Sudo, Toray Industries, Tokyo, Japan	1:10,000
CD133	Rat	eBioscience	1:1000
Ki67	Rabbit	Lab Vision	1:200

Antigen	Conjugation	Source	Dilution
		Secondary antibodies	
Rabbit/Goat/Mouse/Guinea Pig/Rat	Alexa-488	Invitrogen	1:2000
Rabbit/Goat/Mouse/Guinea Pig	Cy3	Jackson ImmunoResearch	1:2000
Rabbit/Goat/Mouse/Guinea Pig/Armenian Hamster	Cy5	Jackson ImmunoResearch	1:500
Rabbit/Goat	Biotinylated	Vector Laboratories	1:250

To quantify the number of lineage-labeled endocrine cells, all endocrine cells on a section were counted and the percentage of endocrine cells expressing YFP determined. For postnatal analyses, the percentage of lineage-labeled endocrine cells was separately quantified within endocrine cell clusters of different sizes. A cluster was defined as a structurally contiguous group of cells. To assess acinar cell neogenesis, all YFP-labeled amylase$^+$ cells on a section were counted. This number was divided by the total amylase$^+$ area measured using Image Pro Plus 5.0.1 software (Media Cybernetics). To account for variations in recombination efficiencies between mice, final values were divided by the recombination efficiency for each mouse and multiplied by 100.

In *Sox9CreER^{T2};R26R^{lacZ}* mice at P21, we counted all β-galactosidase$^+$ cells on three Hematoxylin and Eosin-stained sections per mouse and determined the percentage of β-galactosidase$^+$ cells within the endocrine, acinar or duct cell compartments.

For β-cell mass measurements, pancreata were dissected and separated into head and tail at the point of ligation. A microbalance was used to weigh the tail prior to cryoembedding. The entire tissue sample was sectioned and five sections (800 μm apart) of 10 μm were selected and immunofluorescently stained for insulin. Pictures were taken at 20× magnification and tiled to represent the area of the entire section. The insulin$^+$ area was measured using ImagePro 5.0.1. The autofluorescent signal that is inherent to the tissue was used to determine the total pancreatic tail section area. β-cell mass was calculated by dividing the total insulin$^+$ area by total pancreatic tail tissue area and multiplying this number by the pancreatic tail weight.

Statistical analysis
Statistical significance was determined by two-tailed Student's *t*-test.

RESULTS
Sox9CreER^{T2} mice specifically and efficiently target the embryonic cords and adult pancreatic ducts
To label Sox9$^+$ cells and their descendants we generated BAC transgenic mice in which CreER^{T2} was inserted downstream of the start codon in the first exon of *Sox9* (Fig. 1A). Co-immunofluorescence staining of Sox9 together with CreER demonstrated uniform and specific expression of the CreER transgene exclusively in Sox9$^+$ cells throughout development and adulthood (Fig. 1B,D,I,M). Consistent with the progressive elimination of Sox9 from the tips of the branching epithelium (see Fig. S1A-D in the supplementary material), CreER became gradually excluded from the Ptf1a$^+$ compartment between e12.5 and e14.5 (Fig. 1C,H). Notably, some Ptf1a$^+$ cells still expressed Sox9 and CreER at e14.5 (Fig. 1H, asterisks; Fig. 2B), demonstrating that Sox9$^+$ and Ptf1a$^+$ domains are not entirely distinct at this stage. Unlike Sox9$^+$ cells, Hnf1b$^+$ cells were exclusively found in the trunk region at e14.5 (Fig. 2A) and, accordingly, did not express Ptf1a (Fig. 2C). Triple
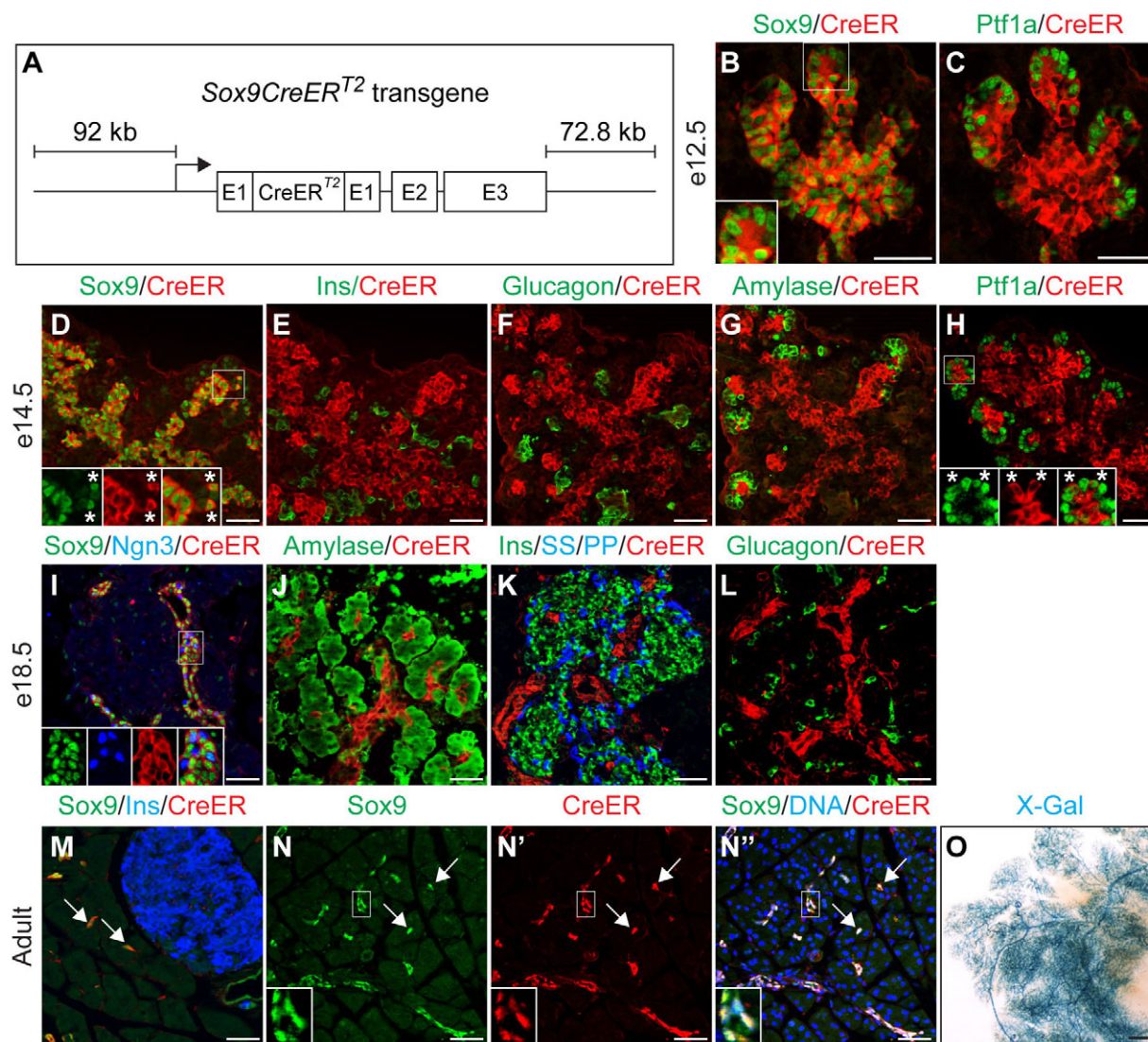
Fig. 1. Sox9CreER^{T2} specifically and efficiently labels Sox9^+ cells in mouse pancreas. (**A**) Schematic of the *Sox9CreER^{T2}* transgene. (**B-N″**) Double and triple immunofluorescent labeling of CreER and various hormones and markers at e12.5, e14.5, e18.5 and P25 (adult). Immunofluorescence analysis for Cre recombinase (CreER) shows specific and uniform expression of CreER in the Sox9^+ domain. Insets and asterisks in B, D and I show Sox9^+ CreER^+ cells (magnification of boxed areas). CreER expression is absent from hormone^+ (E,F,K,L,M) and amylase^+ cells (G,J). CreER expression recedes from Ptf1a^+ tips between e12.5 (C) and e14.5 (H, asterisks in inset show CreER^+ Ptf1a^+ cells). Forty-eight hours after three tamoxifen (TM) injections at P21, CreER is detected in the nucleus (N-N″; insets show magnifications of boxed areas). Arrows in M-N″ point to Sox9/CreER coexpressing terminal duct/centroacinar cells. (**O**) Whole-mount β-galactosidase staining (X-Gal) of *Sox9CreER^{T2};R26R^{lacZ}* mice injected with TM at P10 shows labeling of the entire ductal tree. Scale bars: 50 μm in B-N″; 500 μm in O. Ins, insulin; PP, pancreatic polypeptide; SS, somatostatin.

immunofluorescence staining further revealed a subset of Ptf1a^+ Sox9^+ cells also expressing Nkx6.1 (Fig. 2B), which, together with Pdx1, constitutes the transcriptional code of early multipotent progenitors (Schaffer et al., 2010). These findings suggest that a Sox9^+ Ptf1a^+ Nkx6.1^+ Hnf1b^− zone at the interface between the trunk and tip domains forms a reservoir of multipotent progenitors at later developmental timepoints (Fig. 2D).

Next, to determine whether CreER expression is excluded from differentiated endocrine and acinar cells, we performed co-immunofluorescence staining for CreER together with endocrine and acinar markers. Mirroring the expression pattern of Sox9 (Seymour et al., 2007), CreER was not detected in hormone^+ cells or in cells expressing amylase at any timepoint during development

(Fig. 1E-G,J-L). In the adult pancreas, CreER expression was confined to the ductal tree, including the terminal duct/centroacinar cells (Fig. 1M,N).

To demonstrate that TM mediates translocation of CreER to the nucleus, we generated mice that harbor the *Sox9CreER^{T2}* transgene and the *R26R^{lacZ}* or *R26R^{YFP}* reporter allele and administered TM to induce expression of the *lacZ* or *YFP* reporter gene, respectively. Because recombination occurs between 6 and 48 hours after TM administration (Zhou et al., 2007), we examined pancreata from adult mice 48 hours after TM injection. As anticipated, we found CreER to be nuclear and exclusively localized to Sox9^+ cells (Fig. 1N). TM injection at P10 resulted in efficient X-Gal labeling of the entire ductal tree (Fig. 1O; see Fig. S2A,B in the supplementary
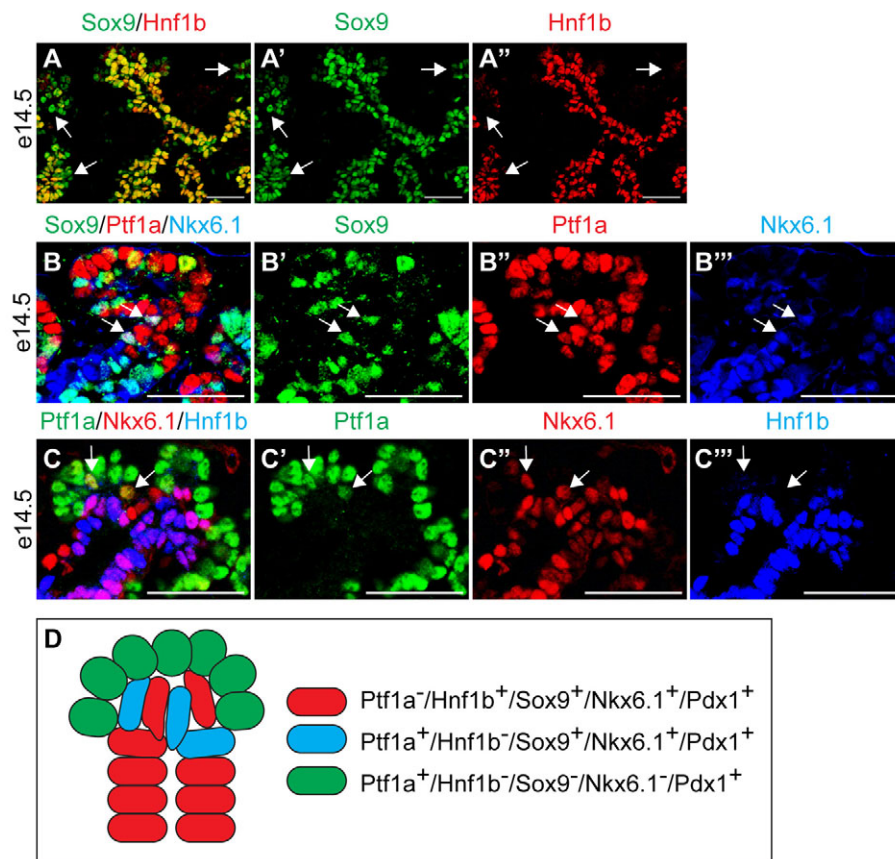
Fig. 2. A Sox9$^+$ Ptf1a$^+$ Nkx6.1$^+$ Hnf1b$^-$ domain marks the distal ends of the embryonic cords of mouse pancreas. (**A-A″**) Immunofluorescence staining reveals that the Sox9$^+$ and Hnf1b$^+$ domains largely coincide at e14.5. However, some Sox9$^+$ cells are Hnf1b$^-$ (arrows). (**B-B‴**) At e14.5, cells coexpress Sox9, Ptf1a and Nkx6.1 (arrows). (**C-C‴**) Ptf1a$^+$ Nkx6.1$^+$ cells in this location do not express Hnf1b (arrows). (**D**) Schematic of different domains in the e14.5 pancreas. Scale bars: 50 μm.

material), whereas no X-Gal labeling was observed in non-injected mice (Fig. 4B). Analysis of pancreatic sections from *Sox9CreER^{T2};R26R^{YFP}* mice further confirmed that recombination occurs in Sox9$^+$ cells throughout the ductal tree (see Fig. S4 in the supplementary material). These results demonstrate that *Sox9CreER^{T2}* mice allow for specific, efficient and inducible labeling of the Sox9$^+$ cell compartment.

To determine how the Sox9$^+$ domain compares with the expression domains of other ductal markers, we examined their extent of overlap with Sox9 in the embryonic and adult pancreas. At e14.5, the Sox9$^+$ domain completely coincided with osteopontin (OPN; Spp1 – Mouse Genome Informatics) (see Fig. S3A in the supplementary material). Mucin-1 (Muc1 – Mouse Genome Informatics) did not mark all Sox9$^+$ cells and was additionally expressed in acinar cells (see Fig. S3A′ in the supplementary material), and *Dolichos biflorus* agglutinin (DBA) staining was restricted to an even smaller subset of Sox9$^+$ cells (see Fig. S3A″ in the supplementary material). In the adult pancreas, Sox9 colocalized with OPN, CD133 (Prom1 – Mouse Genome Informatics), mucin-1, Hes1 and Hnf1b throughout all aspects of the ductal tree, whereas DBA binding was confined to large ducts (see Fig. S4 in the supplementary material). As previously reported (Kopinke and Murtaugh, 2010), mucin-1 was additionally expressed in acinar cells, which are Sox9$^-$ (see Fig. S4D in the supplementary material), whereas OPN also marks endocrine cells (Kilic et al., 2006; data not shown). Our findings show that, especially during development, presumed ductal markers are not expressed in identical cellular domains, implying that these domains could differ in their developmental potential.

Sox9$^+$ cells give rise to endocrine and acinar cells throughout development

Lineage tracing experiments of the Hnf1b$^+$ domain have suggested that the embryonic cords become restricted to an endocrine or duct cell fate by e13.5 (Solar et al., 2009). Because we observed a population of Sox9$^+$ Ptfa1$^+$ Nkx6.1$^+$ Hnf1b$^-$ cells at the distal ends of the embryonic cords (Fig. 2A-D), we tested whether the Sox9$^+$ and Hnf1b$^+$ domains differ in their developmental potential. We injected pregnant dams from intercrosses between *Sox9CreER^{T2}* and *R26R^{YFP}* mice with TM at e14.5 and analyzed *Sox9CreER^{T2};R26R^{YFP}* offspring 24 and 72 hours later (Fig. 3A). Twenty-four hours after TM injection, we observed nuclear CreER exclusively in Sox9$^+$ embryonic cord cells. YFP expression, as a measure of the recombination efficiency, was found in 5-12% of Sox9$^+$ cells (Fig. 3B,C). To measure the extent of acinar and endocrine cell differentiation from the Sox9$^+$ compartment, we assayed whether the relative proportion of lineage-labeled acinar and endocrine cells increased between e15.5 and e17.5. We observed a significant increase in the relative numbers of glucagon$^+$, insulin$^+$ and amylase$^+$ cells labeled with YFP during the chase period (Fig. 3D-I). These findings show that the Sox9$^+$ population produces new endocrine and acinar cells after e14.5, suggesting that the Sox9$^+$ and Hnf1b$^+$ domains have different developmental potential after the secondary transition.

To more fully define the potential of the Sox9$^+$ cell compartment at different embryonic stages, we injected pregnant dams from *Sox9CreER^{T2}* and *R26R^{lacZ}* intercrosses with TM at defined days of embryogenesis and analyzed the respective contribution of lineage-labeled cells to the acinar, ductal and endocrine cell compartments in three-week-old mice (Fig. 4A).
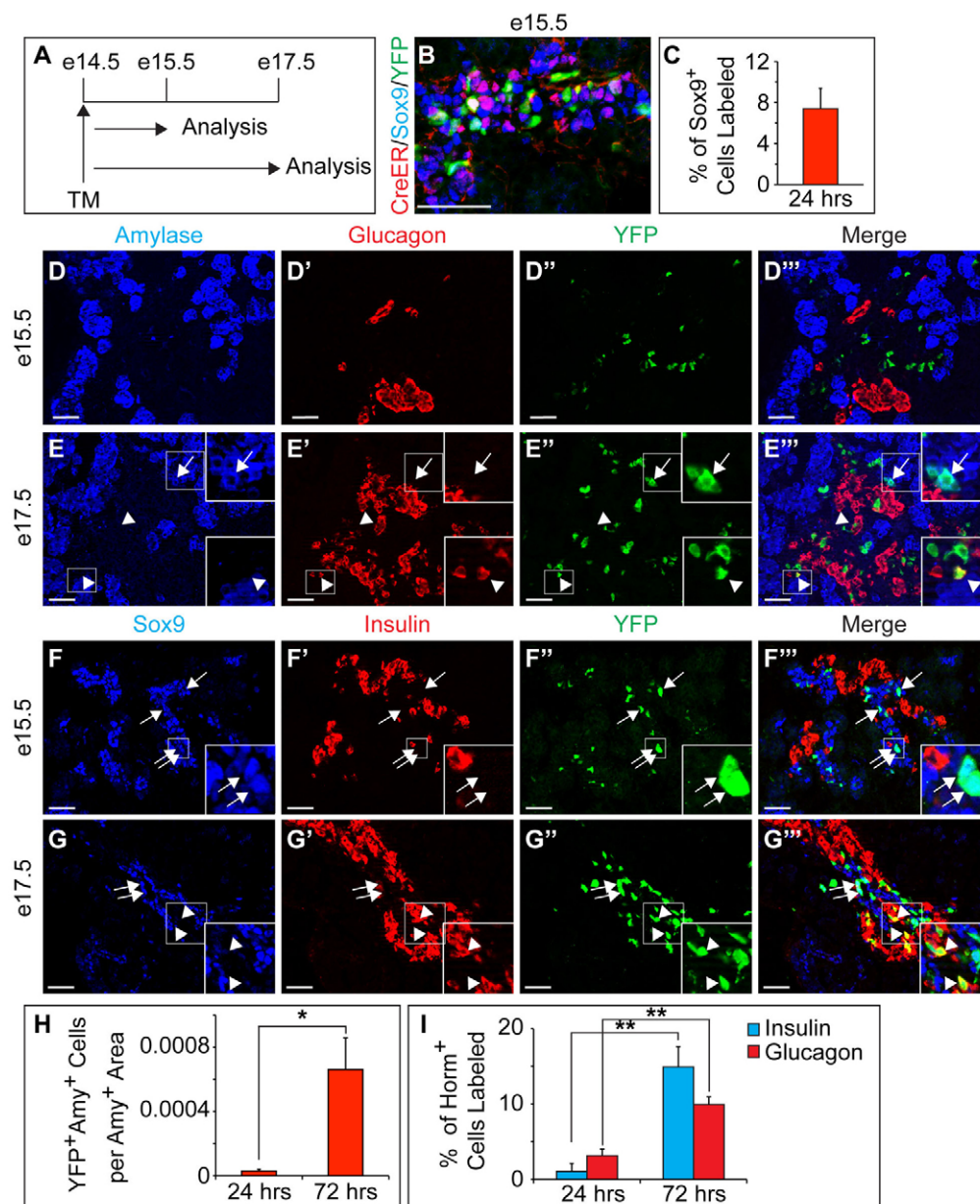
Fig. 3. Sox9+ embryonic cords give rise to endocrine and acinar cells in mouse pancreas. (**A**) Schematic of the lineage tracing experiment in *Sox9CreER^{T2};R26R^{YFP}* mice. Tamoxifen (TM) was administered at e14.5 and pancreatic tissue was analyzed at e15.5 and e17.5. (**B**) Nuclear Cre recombinase (CreER) coincides with YFP in the Sox9+ domain. (**C**) Quantification of YFP+ Sox9+ cells relative to the total number of Sox9+ cells (*n*=3). (**D-G'''**) Immunofluorescence staining for amylase, glucagon and YFP (D-D''',E-E''') or Sox9, insulin and YFP (F-F''',G-G'''). Arrows in E-E''' indicate YFP+ amylase+ cells, arrowheads in E-E''' YFP+ glucagon+ cells and arrowheads in G-G''' YFP+ insulin+ cells. Arrows in F-F''' and G-G''' point to insulin– YFP+ Sox9+ cells. Insets are magnified views of the boxed areas. (**H,I**) Quantification of YFP+ amylase+ cells relative to total amylase+ area (H) or insulin+ or glucagon+ cells relative to the number of total insulin+ or glucagon+ cells (I), respectively (*n*=3). Values are shown as mean ± s.e.m. *$P<0.05$; **$P<0.01$; Amy, amylase; horm, hormone. Scale bars: 50 μm.

When labeled by TM injection at e8.5, Sox9+ progenitor cells gave rise to cells in the acinar, ductal and endocrine cell compartments (Fig. 4C). As lineage tracing experiments based on a *Pdx1CreER^{TM}* transgene have suggested that the Pdx1+ cell population of the e8.5 to e10.5 pancreas is devoid of ductal cell precursors (Gu et al., 2002), the observation that ductal cells arose from early Sox9+ pancreatic progenitors was unexpected. One possible explanation is that ductal progenitors are set aside early and express Sox9 but not Pdx1. This idea is consistent with the finding that, despite extensive overlap, the domains of Sox9 and Pdx1 expression are not identical at e9.0 and Sox9+ Pdx1– cells are also found (Seymour et al., 2007).

When pregnant dams received TM between e12.5 and e18.5, we continued to observe a contribution of Sox9+ cells to acini and ducts, as well as to the endocrine islets (Fig. 4D-G). This indicates that the Sox9+ cell compartment serves as a reservoir for progenitor cells of all pancreatic lineages until birth. To delineate the relative abundance of lineage-labeled cells in each

cell compartment, we quantified the percentage of lineage-labeled acinar, ductal and endocrine cells. As TM was administered at progressively later embryonic timepoints, the percentage of labeled cells increased in ducts but decreased in the acinar cell compartment (Fig. 4H). It is important to note, however, that, given the different proliferative rates of the three pancreatic cell types, this quantification does not provide a direct measure of the relative birth rates of acinar, ductal and endocrine cells from the Sox9+ domain throughout development. Together, these results demonstrate that Sox9+ cells give rise to new acinar and endocrine cells until birth.

A small number of non-β endocrine cells arise from Sox9+ cells during the early postnatal period

To assess the neogenic capacity of Sox9+ cells during the early postnatal period, we injected *Sox9CreER^{T2};R26R^{YFP}* mice at P5 with TM and collected pancreata 2 or 20 days later (Fig. 5A). Two days after TM administration, we observed an average recombination
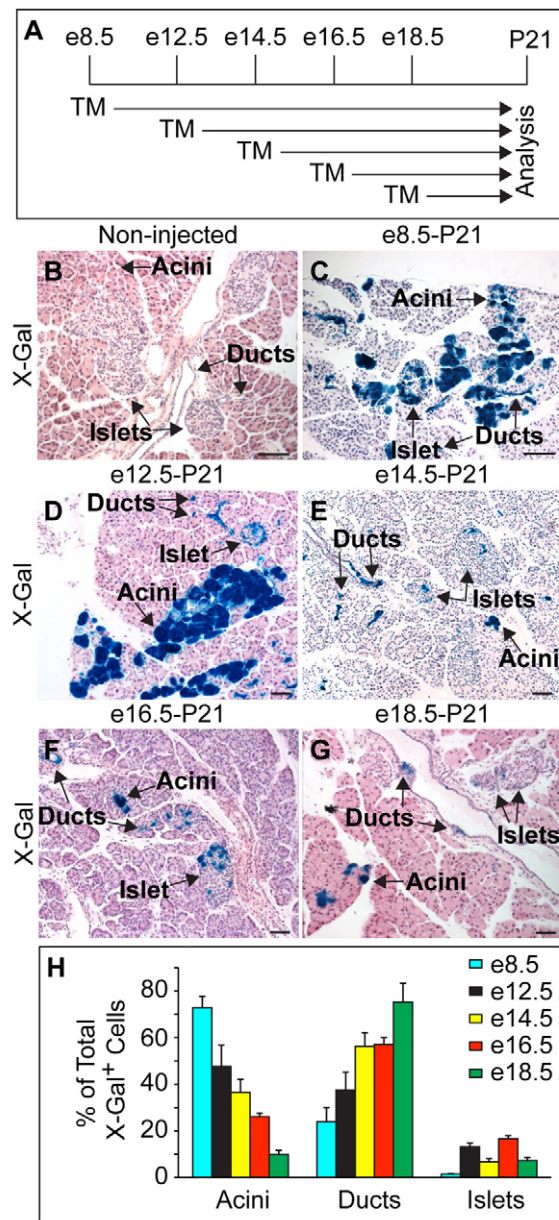
Fig. 4. Endocrine and acinar cells arise from the Sox9^{+} domain throughout development. (**A**) Schematic of the lineage tracing experiment in *Sox9CreER[T2];R26R[lacZ]* mice. Tamoxifen (TM) was administered at various times during embryonic development and pancreatic tissue was analyzed at P21. (**B-G**) Without TM, no β-galactosidase staining (X-Gal) is detected (B). TM injection results in β-galactosidase staining (blue) of acini, ducts and islets at P21 (C-G). (**H**) β-galactosidase^{+} cells were quantified as a percentage of all β-galactosidase [+] cells (labeled as X-Gal[+]; *n*=3) in acini, ducts and islets. Values are shown as mean ± s.e.m. Scale bars: 50 μm.

efficiency of 10% (Fig. 5B,C). To determine whether endocrine or acinar cells arise from the Sox9^{+} compartment between P7 and P25, we compared the proportion of lineage-labeled cells in each cell compartment at these two timepoints (pulse versus chase). At both timepoints, we failed to detect YFP-labeled acinar cells (see Fig. S5A,B,E in the supplementary material), demonstrating that acinar cells do not arise from Sox9^{+} ductal cells during the first three weeks after birth.

Several reports have suggested that postnatal pancreatic ducts are not capable of producing endocrine cells (Means et al., 2008; Solar et al., 2009; Blaine et al., 2010; Kopinke and Murtaugh, 2010). One potential caveat of these studies is that labeled cells were quantified relative to total endocrine area without attention to the size of the endocrine cell clusters. A small contribution to a particular fraction of endocrine cell clusters could, therefore, have been missed. To overcome this limitation, we examined endocrine clusters of different sizes separately for the presence of YFP^{+} cells. Within two days of TM administration, we observed the lineage label preferentially in glucagon[+] or somatostatin[+] pancreatic polypeptide[+] cell clusters with fewer than five cells (Fig. 5D,F,G,I). Compared with non-β islet endocrine cell types, a much smaller percentage of insulin^{+} cells were labeled (Fig. 5J,L). The labeling of endocrine cells shortly after TM administration could reflect either cell neogenesis between P5 and P7 or could be caused by occasional ectopic recombination events in endocrine cells. Although, as described here (Fig. 1K,M), we failed to detect CreER immunoreactivity in endocrine cells, we cannot fully exclude the possibility that some endocrine cells might express low levels of CreER that are below the detection limit of immunofluorescence staining methods but are sufficient to induce recombination. During the 18-day chase period, a small but significant increase in lineage-labeled cells was seen in cell clusters with more than five glucagon[+] or somatostatin[+] pancreatic polypeptide^{+} cells (Fig. 5D-I), whereas the percentage of labeled insulin^{+} cells remained unchanged in clusters of all sizes (Fig. 5J-L). These findings suggest that small numbers of non-β islet endocrine cell types, but not β-cells, continue to arise from Sox9^{+} ductal compartment during the first three postnatal weeks. However, the exceedingly low rate of cell neogenesis from the Sox9^{+} cell compartment also implies that most Sox9^{+} cells no longer function as endocrine progenitors after birth.

Previous studies have failed to detect endocrine cell neogenesis from adult ducts, perhaps because only a small percentage of all ductal cells were labeled (Solar et al., 2009; Kopinke and Murtaugh, 2010; Kushner et al., 2010). To achieve higher recombination efficiencies and to detect possible rare neogenic events from the Sox9^{+} compartment in adult mice, we injected 21-day-old mice with three doses of TM on consecutive days (Fig. 6A). Forty-eight hours after the last TM injection, we detected CreER protein specifically in the Sox9^{+} population (Fig. 1N-N″) and an average of 70% of Sox9^{+} cells were labeled (Fig. 6B,C). With this efficient TM induction regimen we observed occasional labeling of acinar cells (see Fig. S5C,E in the supplementary material), as well as of insulin[+] glucagon[+] and somatostatin[+] pancreatic polypeptide^{+} cells, especially in small endocrine clusters (Fig. 6D,F,G). As the extent of recombination in acinar and endocrine cells correlated with the TM dosage (data not shown), we speculate that some acinar and endocrine cells express low levels of CreER that are below the detection limit of immunofluorescence staining but sufficient to induce recombination in the presence of high TM concentrations. Significantly, our finding that the relative proportion of labeled acinar and endocrine cells stayed constant over the 35-day chase period (see Fig. S5C-E in the supplementary material; Fig. 6D-G) strongly argues that new acinar and endocrine cells do not arise from Sox9^{+} cells in adult mice.

Ngn3^{+} cells arise in Sox9^{+} ducts after partial duct ligation

One highly controversial question is whether or not adult ductal cells generate new β-cells in response to PDL. Using *Sox9CreER[T2]* mice, we induced ductal labeling with high efficiency (Fig. 6A-C)
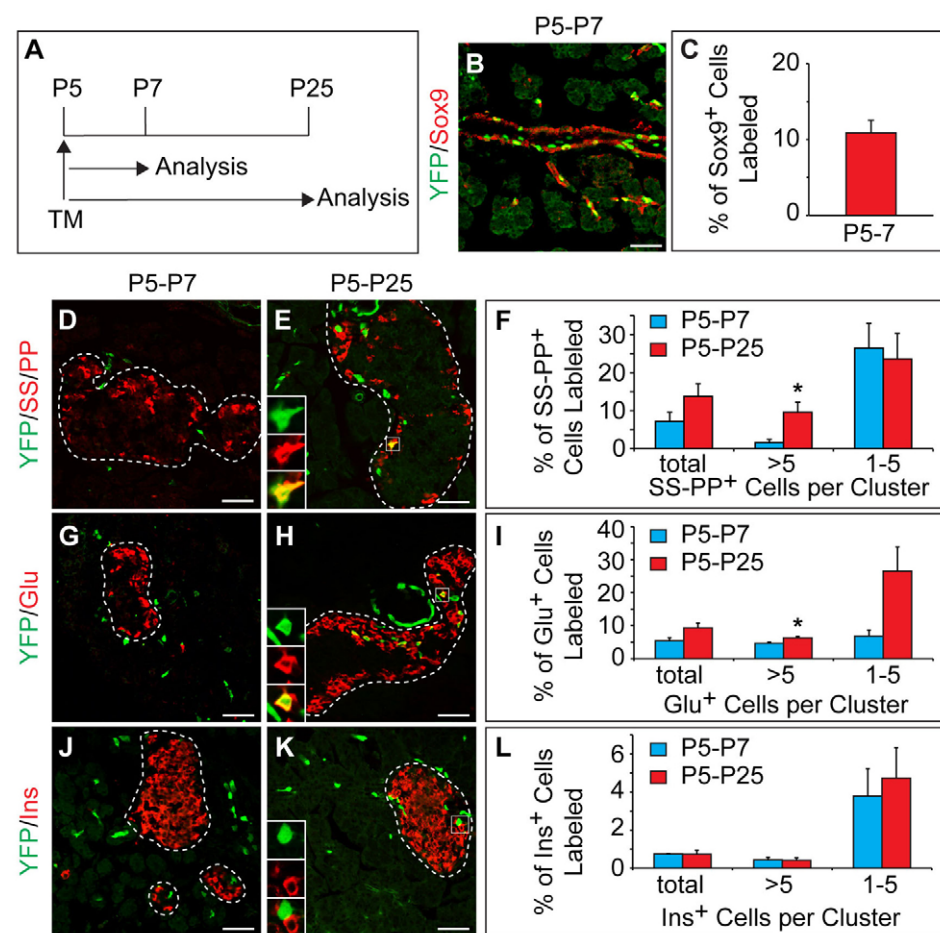
Fig. 5. Small numbers of non-β endocrine cells arise from Sox9+ ducts during the early postnatal period. (**A**) Schematic of the lineage tracing experiment in *Sox9CreER^T2;R26R^YFP* mice. Tamoxifen (TM) was administered at P5 and pancreatic tissue was analyzed at P7 and P25. (**B**) The YFP lineage label is detected primarily in Sox9+ cells. (**C**) Quantification of YFP+ Sox9+ cells relative to the total number of Sox9+ cells (*n*=3). (**D,E,G,H**) Immunofluorescence staining reveals YFP+ SS+ PP+ cells (insets in E) and YFP+ Glu+ cells (insets in H) located in islets (delineated by dashed line). (**J,K**) YFP does not colocalize with insulin (Ins) in islets (insets in K). (**F,I,L**) Quantification of YFP-labeled SS+ PP+ (F), Glu+ (I) or Ins+ (L) cells relative to the total number of SS+ PP+, Glu+ or Ins+ cells, respectively (*n*=3). Values are grouped according to endocrine cell cluster sizes. Values are shown as mean ± s.e.m. *P<0.05. Scale bars: 50 μm. Glu, glucagon; Ins, insulin; PP, pancreatic polypeptide; SS, somatostatin.

and tested whether Ngn3+ and insulin+ cells arose from this cell population after PDL. Mice were injected with three doses of TM at P21, PDL or sham surgery was performed at seven weeks of age, and pancreata were analyzed one and eight weeks after surgery (Fig. 7A).

Based on the observation that PDL induces the expression of *Ngn3* mRNA in the ligated tail within seven days (Xu et al., 2008; Solar et al., 2009), we performed qRT-PCR analysis on pancreatic heads and tails from PDL-treated and control mice. Consistent with previous reports (Xu et al., 2008; Solar et al., 2009), we observed a 40-fold increase in *Ngn3* mRNA levels in the ligated tail (Fig. 7B). Given the recent observation that Ngn3 not only marks endocrine progenitor cells in the embryo but is also expressed in mature islet cells (Wang et al., 2009), we next sought to define which cell types activate Ngn3 expression in response to PDL. In agreement with previous findings (Wang et al., 2009), we detected Ngn3 expression in the majority of islet cells in both PDL- and sham-operated mice (Fig. 7C-E). Co-immmunofluorescence staining for Ngn3 and hormones further revealed that cells of all endocrine subtypes expressed Ngn3 (see Fig. S6A-D in the supplementary material). To distinguish between pre-existing Ngn3+ hormone+ cells and potential duct-derived Ngn3+ cells in the PDL model, we stained pancreas sections for Ngn3 together with hormones, Sox9 and the YFP lineage tracer. This analysis revealed two populations of Ngn3+ cells after PDL: (1) Ngn3+ hormone+ cells with intense immunofluorescence signal for Ngn3, which do not express Sox9 or YFP and largely reside outside ductal

structures. (2) Ngn3+ hormone– cells with lower Ngn3 immunofluorescence signal, residing within Sox9+ YFP-labeled ductules (Fig. 7D,E). As Ngn3+ hormone– cells were not seen in the pancreas of sham-operated mice (Fig. 7C), we conclude that the second Ngn3+ population appears de novo in response to PDL and is derived from the Sox9+ pancreatic ducts. Only a small fraction of YFP+ cells expressed Ngn3, suggesting that Ngn3 activation does not occur in all duct-derived cells.

Surprisingly, examination of the pancreatic heads from ligated mice also revealed, albeit with less frequency, Ngn3+ hormone– Sox9+ YFP+ cells located in small ductules (Fig. 7E). These findings indicate that PDL causes a response not only in the tail distal to the ligation but also in the proximal head region. To better quantify which cells activate *Ngn3* in response to PDL, we compared *Ngn3* and *Sox9* mRNA levels in FACS-isolated *Sox9CreER*-lineage-labeled cells from head and tail regions of both PDL- and sham-operated mice. For comparison, we also included RNA from isolated islets. As expected, *Sox9* was highly enriched in ductal cells compared with islets and was induced in response to PDL (Fig. 7F). mRNA for *Ngn3* was four- or ninefold more abundant in islets than in duct-derived cells of the ligated tail or head, respectively (Fig. 7F). This is consistent with our finding that Ngn3 is expressed only in a subset of duct-derived cells, whereas the majority of islet cells expressed Ngn3. Furthermore, PDL resulted in a twofold increase in *Ngn3* mRNA levels in the lineage-labeled population of the ligated tail compared with YFP+ cells isolated from sham-operated mice. Comparison of *Ngn3* mRNA
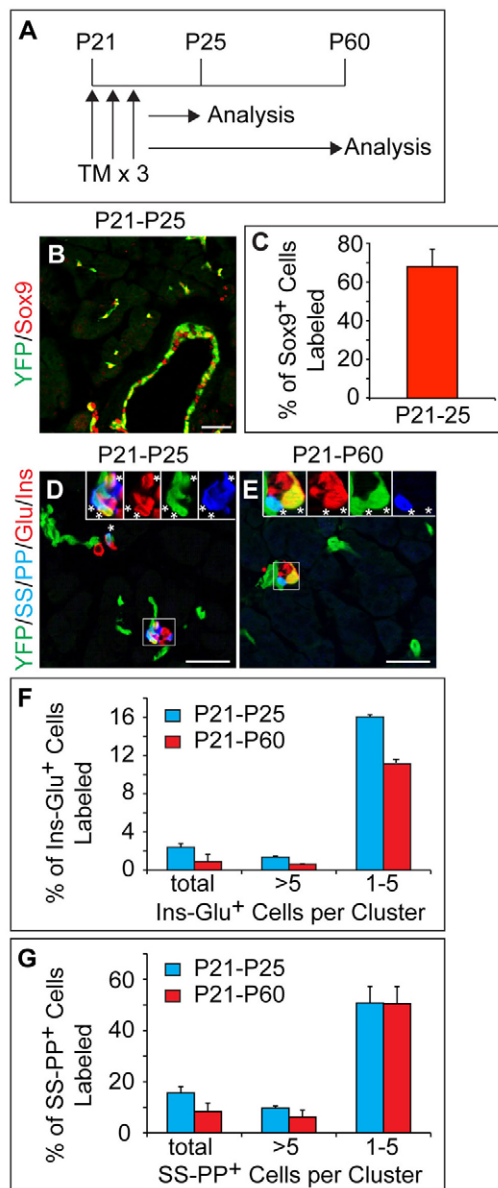
Fig. 6. Endocrine cells do not arise from Sox9+ ducts during adulthood. (**A**) Schematic of the lineage tracing experiment in *Sox9CreER^T2^;R26R^YFP^* mice. Tamoxifen (TM) was administered daily for three days beginning at postnatal day P21 and pancreatic tissue was analyzed at P25 and P60. (**B**) The YFP lineage label is primarily detected in Sox9+ cells. (**C**) Quantification of YFP+ Sox9+ cells relative to the total number of Sox9+ cells (*n*=3). (**D,E**) Immunofluorescence staining reveals YFP+ SS+ PP+ cells and YFP+ Ins+ Glu+ cells closely associated with YFP+ ducts at P25 (insets in D) and P60 (insets in E). Asterisks indicate YFP+ hormone+ cells. (**F,G**) Quantification of YFP-labeled Ins+ Glu+ (F) or SS+ PP+ (G) cells relative to the total number of Ins+ Glu+ or SS+ PP+ cells, respectively (*n*=3). Values are grouped according to endocrine cell cluster sizes. Values are shown as mean ± s.e.m. Scale bars: 50 μm. Glu, glucagon; Ins, insulin; PP, pancreatic polypeptide; SS, somatostatin.

levels in islets from control and PDL-treated mice further revealed a larger overall increase in *Ngn3* expression in islets than in ducts (Fig. 7G). Overall, our findings demonstrate that PDL results in a measurable, but modest, induction of *Ngn3* expression in duct-derived cells.

Duct-derived cells do not contribute to the β-cell compartment after partial duct ligation

To assess whether PDL-induced duct-derived Ngn3+ cells activate endocrine differentiation programs, we examined if these cells express the key endocrine differentiation factors Pdx1, Nkx6.1 and Pax6. In sham-operated mice, we detected a low immunofluorescent signal for Pdx1 in some Sox9+ ductal cells (Fig. 8A) but found Nkx6.1 and Pax6 expression to be entirely confined to islet cells (Fig. 8D,G). After PDL, Pdx1 was detected in the majority of duct-derived cells of the tail and head region, including Ngn3+ cells (Fig. 8B,C), but PDL failed to induce Nkx6.1 or Pax6 expression in duct-derived Ngn3+ cells (Fig. 8E,F,H,I).

Next, we tested directly whether PDL-induced Sox9+ Ngn3+ cells progress to form β-cells. Given our observation that PDL activates Ngn3 in some Sox9+ cells of the head region (Fig. 7E), we used pancreatic tails from sham-operated mice as controls. We frequently detected small clusters of insulin+ cells abutting lineage-labeled ductal structures (Fig. 9B), but observed virtually no colocalization of YFP with insulin in either PDL-treated or control mice (Fig. 9A-C). In tails from mice isolated seven days after PDL, we identified a total of only 20 insulin+ YFP+ cells out of the 23,488 β-cells that were counted, which was almost identical to the observed 26 insulin+ YFP+ cells out of 20,046 insulin+ cells in sham-operated control mice (see Table S1 in the supplementary material). The contribution of lineage-labeled cells to the β-cell compartment was independent of labeling efficiency, which ranged from 46.3% to 84.5% in the PDL-treated cohort (data not shown). To determine whether β-cells arise from Sox9+ ductal cells at later timepoints after PDL, we also analyzed mice eight weeks after PDL. The numbers of lineage-labeled insulin+ cells were similar to the numbers one week after PDL and revealed no difference between PDL-treated and control mice (Fig. 9C; Table S1 in the supplementary material). Together, these analyses suggest that duct-derived Ngn3+ cells do not progress to form new endocrine cells in the PDL model.

As it has been suggested that PDL induces de novo formation of small endocrine cell clusters (Wang et al., 1995; Xu et al., 2008), we next compared the number of β-cells located in small clusters in PDL-treated and sham-operated mice seven days after surgery. Consistent with our finding that β-cells do not arise from ducts after PDL, we also failed to observe a significant increase in small β-cell clusters (see Table S1 in the supplementary material).

To investigate more rigorously whether new β-cells are generated after PDL, we quantified β-cell mass as this parameter has been used in previous studies to assess PDL-induced β-cell regeneration (Xu et al., 2008; Solar et al., 2009). In these studies, β-cell mass was determined by dividing the morphometrically measured insulin+ area by total section area, which was then multiplied by pancreatic weight. Applying this method, we observed an approximately threefold increase in β-cell mass one week after PDL (see Fig. S7A,B in the supplementary material), thus confirming previous findings (Xu et al., 2008; Solar et al., 2009). However, given the drastic PDL-induced changes in tissue composition, we questioned whether these tissue area-based measurements are suited to appropriately assess changes in β-cell numbers in the PDL model. Within seven days, PDL results in acute pancreatitis, marked by tissue edema, fatty degeneration, fibrosis and an almost complete loss of acinar tissue (Yeo et al., 1989; Sakaguchi et al., 2006). Consistent with the loss of acinar tissue, we observed a significant reduction in total tail section area one week after PDL (13.7×10^6 μm² per
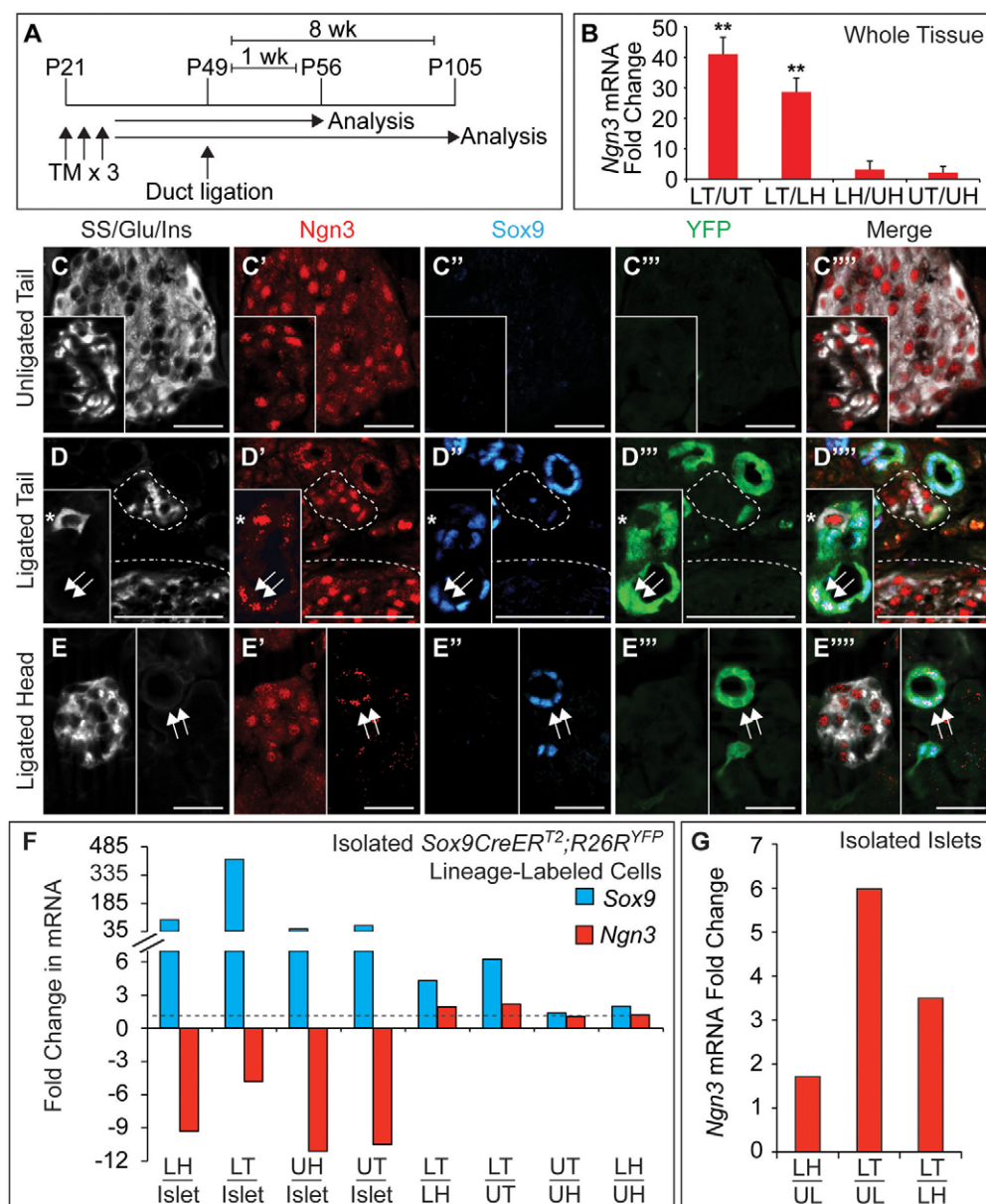
DEVELOPMENT

Fig. 7. Ngn3 expression is induced in duct-derived cells and islets after partial duct ligation (PDL). (**A**) Schematic of the lineage tracing experiment in *Sox9CreER^T2^;R26R^YFP^* mice. Tamoxifen (TM) was administered daily for three days beginning at P21, duct ligation or sham-operation was performed at P49 and pancreatic tissue was analyzed one or eight weeks later. (**B**) Quantitative RT-PCR analysis of pancreatic heads and tails isolated from mice one week after sham-operation or PDL (*n*=5). (**C-E''''**) Immunofluorescence staining for somatostatin (SS), glucagon (Glu) and insulin (Ins) together with Ngn3, Sox9 and YFP reveals Ngn3 in endocrine cells in pancreatic tails of sham-operated mice (C-C'''') and tails (D-D'''', dashed lines delineate endocrine cell clusters) and heads (E-E'''') of mice seven days after PDL. Hormone+ Ngn3+ cells in ducts are YFP– Sox9– (asterisks in D-D''''). After PDL, Ngn3 is expressed in YFP+ Sox9+ cells of the ligated tail (arrows in D-D'''') and head (arrows in E-E''''). (**F,G**) Quantitative RT-PCR analysis of YFP+ cells (F, *n*=4) or islets (G, *n*=6) isolated from mice one week after sham-operation or PDL. Values are shown as mean ± s.e.m. **P<0.01. LH, ligated head; LT, ligated tail; UH, unligated head; UT, unligated tail; UL, unligated whole pancreas. Scale bars: 50 μm.

section in control mice versus 3.7×10^6 μm² per section in PDL-treated mice; *n*=5; see Fig. S7C,D in the supplementary material). One might assume that the loss of the acinar compartment will be corrected for in final β-cell mass measurements by multiplying the ratio of the areas by the weight of the pancreatic tail. However, this assumption fails to take into account the fact that the tissue edema and fatty degeneration contribute to the weight of the tail but are not accounted for in the area measurements (see Fig. S7D in the supplementary material). The PDL-induced changes in tissue composition therefore skew results and suggest increased β-cell mass even if β-cell numbers are unchanged. Significantly, this argues that β-cell mass measurements based on tissue area and weight do not provide an accurate measure of changes in β-cell numbers in response to PDL. To acquire an additional measure of β-cell mass before and after PDL, we determined total pancreatic insulin content in ligated and sham-operated mice. Importantly, we opted to not normalize insulin content measurements to the

amount of total pancreatic protein, as this would once again result in inaccurate measurements due to the loss of acinar cells after PDL. Rather, we normalized by mouse weight and found that total pancreatic insulin content did not change in response to PDL (Fig. 9D). Our combined evidence that the numbers of insulin+ cells in small clusters and insulin content do not change in response to PDL raises the possibility that PDL does not induce significant β-cell regeneration and illustrates the need for developing additional methods to assess changes in β-cell mass after pancreatic injury.

DISCUSSION

We present here a detailed fate analysis of the pancreatic Sox9+ domain during embryonic development, adulthood and in response to pancreatic injury by PDL. By identifying the Sox9+ domain as a progenitor compartment for endocrine and acinar cells throughout embryogenesis, we demonstrate that both endocrine and acinar cells are generated through a neogenic process until birth.
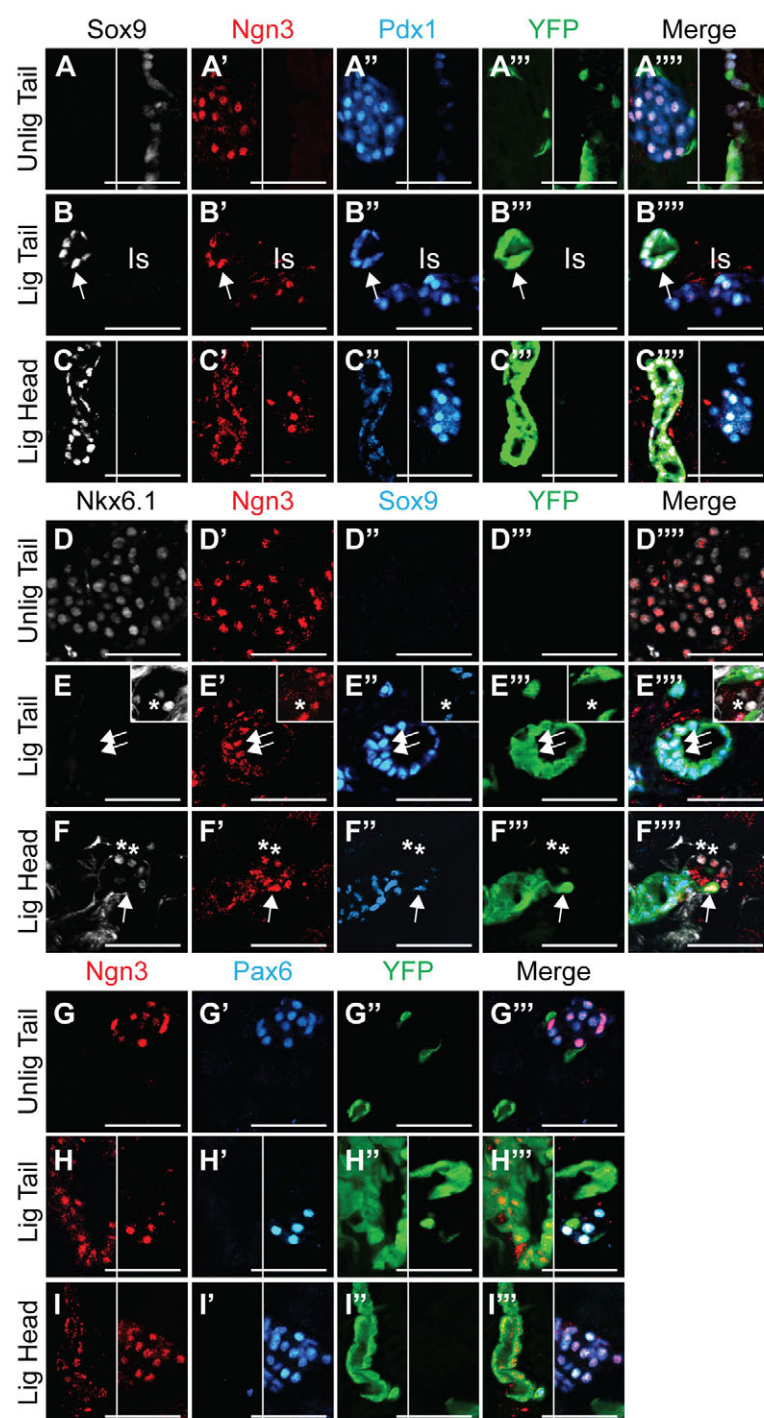
Fig. 8. Duct-derived Ngn3+ Sox9+ cells after partial duct ligation (PDL) express Pdx1 but not Nkx6.1 and Pax6. (**A-I'''**) Immunofluorescence staining of pancreata from PDL-treated or sham-operated *Sox9CreER^T2;R26R^YFP* mice reveals cells expressing Ngn3 together with Pdx1 (A-C''''), Nkx6.1 (D-F'''') or Pax6 (G-I''') in pancreatic tails of sham-operated (A-A'''',D-D'''',G-G''') and tails (B-B'''',E-E'''',H-H''') and heads (C-C'''',F-F'''',I-I''') of PDL-treated mice one week after surgery. A subset of YFP+ Sox9+ cells in tails of sham-operated mice express Pdx1 (A-A'''') but not Nkx6.1 (D-D'''') or Pax6 (G-G'''). Ngn3+ YFP− Sox9− cells are also found in the pancreatic tails and heads of PDL-treated mice (asterisks in E-F'''' mark Ngn3+ Nkx6.1+ YFP− Sox9− cells). Ngn3+ YFP+ Sox9+ cells after PDL express Pdx1 (arrows in B-B'''') but not Nkx6.1 (arrows in E-F'''') or Pax6 (H-I'''). Unlig Tail, unligated tail; Lig Tail, ligated tail; Lig Head, ligated head; Is, islet. Scale bars: 50 µm.

Furthermore, we show that during the early postnatal period a limited number of endocrine cells continue to arise from Sox9+ ducts. Finally, we identify Sox9+ duct cells as progenitors of Ngn3+ cells, but not β-cells, after PDL. Our findings suggest that PDL partially initiates a program of endocrine cell differentiation in ducts but that the adult pancreatic environment does not support completion of the differentiation pathway.

Recent studies have shown that during embryonic development pancreatic progenitors become progressively restricted in their lineage potential (Zhou et al., 2007; Solar et al., 2009; Schaffer et al., 2010). Fate-mapping studies of the tip and trunk compartments

have suggested that acinar cells arise from progenitors only up until e14 (Zhou et al., 2007; Solar et al., 2009), implying that subsequent expansion of the acinar compartment occurs exclusively by proliferation of pre-existing acinar cells. These conclusions were based on tracing Hnf1b+ trunk cells, a domain that has been suggested to fully coincide with the Sox9+ domain (Solar et al., 2009). Although we confirmed that the Sox9+ and Hnf1b+ domains are identical in the adult pancreas, we found that in the embryo Sox9 marks a population of cells at the interface of the tip and trunk domains that expresses Ptf1a and Nkx6.1 but not Hnf1b. Because Ptf1a becomes excluded from trunk progenitors that
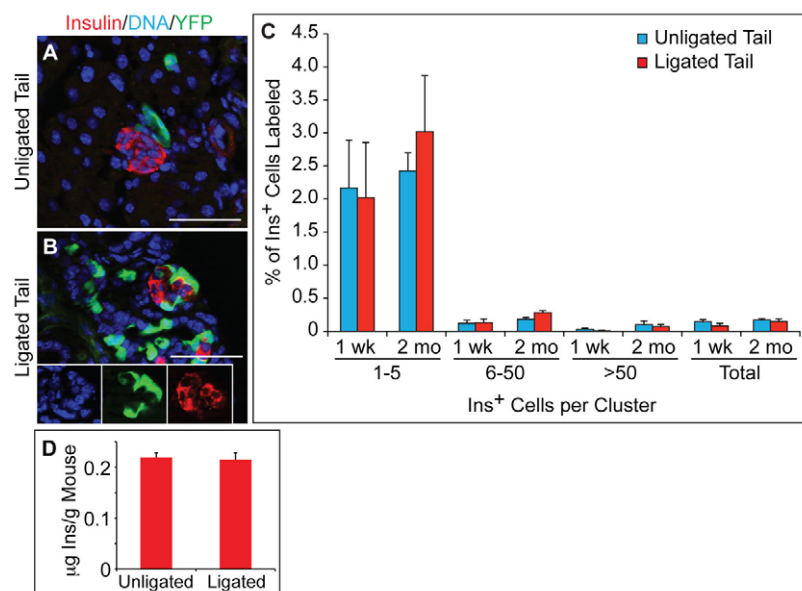
Fig. 9. Sox9⁺ cells do not give rise to insulin⁺ cells after partial duct ligation (PDL).
(**A,B**) Immunofluorescence analysis of pancreatic tails from PDL-treated or sham-operated *Sox9CreER^{T2};R26R^{YFP}* mice for insulin and YFP. (**C**) Quantification of YFP⁺ insulin⁺ cells relative to the total number of insulin⁺ cells shows no increase in the percentage of YFP⁺ β-cells one week (1 wk; $n=4$) or two months (2 mo; $n=3$) after PDL. Values are shown for all insulin⁺ cells (total) and for insulin⁺ cell clusters of different sizes. (**D**) Whole pancreas insulin content relative to body weight ($n=10$). Values are shown as mean ± s.e.m. Ins, insulin. Scale bars: 50 µm.

undergo endocrine/ductal fate commitment but is coexpressed with Nkx6.1 and Sox9 in multipotent progenitors (Schaffer et al., 2010), this transcriptional signature suggests that these cells are uncommitted multipotent progenitors. Consistent with this idea, we found that Sox9⁺ cells generated cells of all pancreatic lineages, including acinar cells, throughout embryogenesis.

Interestingly, our study demonstrates that duct cells continue to undergo non-β endocrine cell neogenesis at a low rate for the first three weeks after birth. In contrast with our study, fate-mapping studies of the *CK19-*, *Hnf1b-* and *mucin-1*-ductal domains failed to detect a contribution of ductal cells to the endocrine compartment during early postnatal life (Means et al., 2008; Solar et al., 2009; Kopinke and Murtaugh, 2010). As these studies analyzed lineage-labeled cells exclusively as a percentage of total endocrine area, but not of endocrine clusters of different sizes, it is possible that a small but significant contribution of ductal cells was not detected. Alternatively, the potential to undergo endocrine cell differentiation could be limited to only a subset of ductal cells that is not uniformly labeled by all ductal markers. This possibility is consistent with a recent study showing that only terminal ducts, which express Sox9 but not CK19, contain a population of cells with colony-forming activity and the potential of generating endocrine cells (Rovira et al., 2010). In contrast with our study, lineage tracing of ducts with a *CAIICre* transgene revealed β-cell neogenesis during the postnatal period (Inada et al., 2008). However, as the *CAIICre* transgene is constitutively expressed, it is possible that recombination occurred prior to birth, when β-cells still arise from ducts.

Although recent studies have shown that PDL induces the generation of endocrine differentiation-competent Ngn3⁺ cells (Xu et al., 2008), the cellular origin of these cells has remained elusive. Our findings show that PDL induces Ngn3 expression in both duct-derived cells and endocrine cells but that ductal cells do not differentiate into endocrine cells. Duct-derived Ngn3⁺ cells displayed lower levels of Ngn3 than endocrine islets, expressed Sox9 but not hormones, and were only observed after PDL. The absence of the pre-endocrine markers Nkx6.1 and Pax6 in duct-derived Ngn3⁺ cells provides further support for the conclusion that endocrine cell neogenesis is not initiated in ducts. Our findings are in agreement with a recent study by Solar et al. (Solar et al., 2009),

who reported a lack of β-cell neogenesis from ducts seven days after PDL when using *Hnf1bCreER* mice to trace ductal cells. Similarly, lineage tracing experiments in a TGFα-induced pancreatitis model showed that duct-associated insulin⁺ cells did not arise from hyperplastic ducts (Blaine et al., 2010). Combined evidence from these studies suggests that pancreatitis, whether induced by PDL or other stimuli, is not sufficient to induce β-cell regeneration from ducts.

Our study confirms previous findings by Gu and colleagues that Ngn3 is expressed in the islet (Wang et al., 2009). We further demonstrate that Ngn3 is expressed in the majority of β-cells as well as in the other endocrine cell types. Consistent with expression of Ngn3 in endocrine cells, Xu et al. also detected insulin and glucagon in GFP⁺ cells isolated from PDL-treated *Ngn3GFP* transgenic mice (Xu et al., 2008). Because GFP protein is very stable, Xu et al. interpreted this as evidence for ductal cells progressively moving from an Ngn3⁺ hormone⁻ into an Ngn3⁻ hormone⁺ state. Given the absence of ductal lineage tracing to endocrine cells after PDL, an alternative explanation for their finding is that *Ngn3GFP*-based cell sorting resulted in the isolation of pre-existing islet cells as well as duct-derived Ngn3⁺ cells. This could also explain why *Ngn3* transcripts were found in both the hormone⁺ and hormone⁻ fraction of the Ngn3GFP population. The presence of Ngn3 in β-cells also suggests an alternative interpretation for the finding that shRNA-mediated inhibition of *Ngn3* activity after PDL decreased β-cell mass (Xu et al., 2008). It is possible that reduced Ngn3 activity in islets inhibits PDL-induced β-cell proliferation (Wang et al., 1995; Xu et al., 2008), a notion that is directly supported by Xu's observation that lentivirus-mediated *Ngn3* inhibition reduced BrdU incorporation into β-cells (Xu et al., 2008).

Although increased β-cell proliferation after PDL has been suggested to contribute to the expansion of the β-cell population, these gains in β-cell mass might be offset by the simultaneous induction of β-cell apoptosis (Wang et al., 1995; Xu et al., 2008). This raises the question of whether β-cells regenerate in the PDL model. In the results section, we have explained why the PDL-induced tissue edema renders morphometry-based β-cell mass measurements inaccurate for assessing changes in β-cell mass after PDL (see Fig. S7 in the supplementary material). We note that

previous conclusions that new β-cells are generated after PDL are all based on morphometric measurements of β-cell mass (Xu et al., 2008; Solar et al., 2009). Our finding that whole pancreas insulin content does not increase after PDL raises the possibility that the β-cell compartment does not expand in response to PDL. Consistent with our results, a previous study also reported no increase in insulin content per pancreas after PDL (Wang et al., 1995). However, as it is possible that PDL regulates insulin expression, a definitive answer to the question of whether or not β-cell mass increases in response to PDL will have to await FACS-based or optical methods suited to accurately measure β-cell numbers and mass in the entire organ.

Competing interests statement
The authors declare no competing financial interests.

Supplementary material
Supplementary material for this article is available at
http://dev.biologists.org/lookup/suppl/doi:10.1242/dev.056499/-/DC1

References
Akiyama, H., Kim, J. E., Nakashima, K., Balmes, G., Iwai, N., Deng, J. M., Zhang, Z., Martin, J. F., Behringer, R. R., Nakamura, T. et al. (2005). Osteo-chondroprogenitor cells are derived from Sox9 expressing precursors. *Proc. Natl. Acad. Sci. USA* **102**, 14665-14670.

Blaine, S. A., Ray, K. C., Anunobi, R., Gannon, M. A., Washington, M. K. and Means, A. L. (2010). Adult pancreatic acinar cells give rise to ducts but not endocrine cells in response to growth factor signaling. *Development* **137**, 2289-2296.

Cheung, M. and Briscoe, J. (2003). Neural crest development is regulated by the transcription factor Sox9. *Development* **130**, 5681-5693.

Chung, C. H., Hao, E., Piran, R., Keinan, E. and Levine, F. (2010). Pancreatic beta-cell neogenesis by direct conversion from mature alpha-cells. *Stem Cells* **28**, 1630-1638.

Dor, Y., Brown, J., Martinez, O. I. and Melton, D. A. (2004). Adult pancreatic beta-cells are formed by self-duplication rather than stem-cell differentiation. *Nature* **429**, 41-46.

Garcia-Lavandeira, M., Quereda, V., Flores, I., Saez, C., Diaz-Rodriguez, E., Japon, M. A., Ryan, A. K., Blasco, M. A., Dieguez, C., Malumbres, M. et al. (2009). A GRFa2/Prop1/stem (GPS) cell niche in the pituitary. *PLoS One* **4**, e4815.

Gu, D. and Sarvetnick, N. (1993). Epithelial cell proliferation and islet neogenesis in IFN-g transgenic mice. *Development* **118**, 33-46.

Gu, G., Dubauskaite, J. and Melton, D. A. (2002). Direct evidence for the pancreatic lineage: NGN3+ cells are islet progenitors and are distinct from duct progenitors. *Development* **129**, 2447-2457.

Henseleit, K. D., Nelson, S. B., Kuhlbrodt, K., Hennings, J. C., Ericson, J. and Sander, M. (2005). NKX6 transcription factor activity is required for alpha- and beta-cell development in the pancreas. *Development* **132**, 3139-3149.

Inada, A., Nienaber, C., Katsuta, H., Fujitani, Y., Levine, J., Morita, R., Sharma, A. and Bonner-Weir, S. (2008). Carbonic anhydrase II-positive pancreatic cells are progenitors for both endocrine and exocrine pancreas after birth. *Proc. Natl. Acad. Sci. USA* **105**, 19915-19919.

Kawaguchi, Y., Cooper, B., Gannon, M., Ray, M., MacDonald, R. J. and Wright, C. V. (2002). The role of the transcriptional regulator Ptf1a in converting intestinal to pancreatic progenitors. *Nat. Genet.* **32**, 128-134.

Kilic, G., Wang, J. and Sosa-Pineda, B. (2006). Osteopontin is a novel marker of pancreatic ductal tissues and of undifferentiated pancreatic precursors in mice. *Dev. Dyn.* **235**, 1659-1667.

Kopinke, D. and Murtaugh, L. C. (2010). Exocrine-to-endocrine differentiation is detectable only prior to birth in the uninjured mouse pancreas. *BMC Dev. Biol.* **10**, 38.

Kushner, J. A., Weir, G. C. and Bonner-Weir, S. (2010). Ductal origin hypothesis of pancreatic regeneration under attack. *Cell Metab.* **11**, 2-3.

Means, A. L., Xu, Y., Zhao, A., Ray, K. C. and Gu, G. (2008). A CK19(CreERT) knockin mouse line allows for conditional DNA recombination in epithelial cells in multiple endodermal organs. *Genesis* **46**, 318-323.

Pfaffl, M. W. (2001). A new mathematical model for relative quantification in real-time RT-PCR. *Nucleic Acids Res.* **29**, e45.

Pictet, R. and Rutter, W. J. (1972). Development of the embryonic endocrine pancreas. In *Handbook of Physiology* (eds A. P. Society, D. F. Steiner and N. Frenkel), pp. 25-66. Washington DC: Williams and Wilkins.

Rovira, M., Scott, S. G., Liss, A. S., Jensen, J., Thayer, S. P. and Leach, S. D. (2010). Isolation and characterization of centroacinar/terminal ductal progenitor cells in adult mouse pancreas. *Proc. Natl. Acad. Sci. USA* **107**, 75-80.

Sakaguchi, Y., Inaba, M., Kusafuka, K., Okazaki, K. and Ikehara, S. (2006). Establishment of animal models for three types of pancreatitis and analyses of regeneration mechanisms. *Pancreas* **33**, 371-381.

Schaffer, A. E., Freude, K. K., Nelson, S. B. and Sander, M. (2010). Nkx6 transcription factors and Ptf1a function as antagonistic lineage determinants in multipotent pancreatic progenitors. *Dev. Cell* **18**, 1022-1029.

Seymour, P. A., Bennett, W. R. and Slack, J. M. (2004). Fission of pancreatic islets during postnatal growth of the mouse. *J. Anat.* **204**, 103-116.

Seymour, P. A., Freude, K. K., Tran, M. N., Mayes, E. E., Jensen, J., Kist, R., Scherer, G. and Sander, M. (2007). SOX9 is required for maintenance of the pancreatic progenitor cell pool. *Proc. Natl. Acad. Sci. USA* **104**, 1865-1870.

Seymour, P. A., Freude, K. K., Dubois, C. L., Shih, H. P., Patel, N. A. and Sander, M. (2008). A dosage-dependent requirement for Sox9 in pancreatic endocrine cell formation. *Dev. Biol.* **323**, 19-30.

Solar, M., Cardalda, C., Houbracken, I., Martin, M., Maestro, M. A., De Medts, N., Xu, X., Grau, V., Heimberg, H., Bouwens, L. et al. (2009). Pancreatic exocrine duct cells give rise to insulin-producing beta cells during embryogenesis but not after birth. *Dev. Cell* **17**, 849-860.

Soriano, P. (1999). Generalized lacZ expression with the ROSA26 Cre reporter strain. *Nat. Genet.* **21**, 70-71.

Srinivas, S., Watanabe, T., Lin, C. S., William, C. M., Tanabe, Y., Jessell, T. M. and Costantini, F. (2001). Cre reporter strains produced by targeted insertion of EYFP and ECFP into the ROSA26 locus. *BMC Dev. Biol.* **1**, 4.

Vidal, V. P., Chaboissier, M. C., Lutzkendorf, S., Cotsarelis, G., Mill, P., Hui, C. C., Ortonne, N., Ortonne, J. P. and Schedl, A. (2005). Sox9 is essential for outer root sheath differentiation and the formation of the hair stem cell compartment. *Curr. Biol.* **15**, 1340-1351.

Wang, R. N., Kloppel, G. and Bouwens, L. (1995). Duct- to islet-cell differentiation and islet growth in the pancreas of duct-ligated adult rats. *Diabetologia* **38**, 1405-1411.

Wang, R. N., Bouwens, L. and Kloppel, G. (1996). Beta-cell growth in adolescent and adult rats treated with streptozotocin during the neonatal period. *Diabetologia* **39**, 548-557.

Wang, S., Jensen, J. N., Seymour, P. A., Hsu, W., Dor, Y., Sander, M., Magnuson, M. A., Serup, P. and Gu, G. (2009). Sustained Neurog3 expression in hormone-expressing islet cells is required for endocrine maturation and function. *Proc. Natl. Acad. Sci. USA* **106**, 9715-9720.

Xu, G., Stoffers, D. A., Habener, J. F. and Bonner-Weir, S. (1999). Exendin-4 stimulates both beta-cell replication and neogenesis, resulting in increased beta-cell mass and improved glucose tolerance in diabetic rats. *Diabetes* **48**, 2270-2276.

Xu, X., D'Hoker, J., Stange, G., Bonne, S., De Leu, N., Xiao, X., Van de Casteele, M., Mellitzer, G., Ling, Z., Pipeleers, D. et al. (2008). Beta cells can be generated from endogenous progenitors in injured adult mouse pancreas. *Cell* **132**, 197-207.

Yeo, C. J., Bastidas, J. A., Schmieg, R. E., Jr., Walfisch, S., Couse, N. F., Olson, J. L., Andersen, D. K. and Zinner, M. J. (1989). Pancreatic structure and glucose tolerance in a longitudinal study of experimental pancreatitis-induced diabetes. *Ann. Surg.* **210**, 150-158.

Zhou, Q., Law, A. C., Rajagopal, J., Anderson, W. J., Gray, P. A. and Melton, D. A. (2007). A multipotent progenitor domain guides pancreatic organogenesis. *Dev. Cell* **13**, 103-114.

DEVELOPMENT